Random cohort effects and age groups dependency structure for mortality modelling and forecasting: Mixed-effects time-series model approach

Ka Kin Lam, Bo Wang

School of Mathematics and Actuarial Science, University of Leicester, Leicester LE1 7RH, UK

Abstract

There have been significant efforts devoted to solving the longevity risk given that a continuous growth in population ageing has become a severe issue for many developed countries over the past few decades. The Cairns-Blake-Dowd (CBD) model, which incorporates cohort effects parameters in its parsimonious design, is one of the most well-known approaches for mortality modelling at higher ages and longevity risk. This article proposes a novel mixed-effects time-series approach for mortality modelling and forecasting with considerations of age groups dependence and random cohort effects parameters. The proposed model can disclose more mortality data information and provide a natural quantification of the model parameters uncertainties with no pre-specified constraint required for estimating the cohort effects parameters. The abilities of the proposed approach are demonstrated through two applications with empirical male and female mortality data. The proposed approach shows remarkable improvements in terms of forecast accuracy compared to

^{*}Corresponding author. E-mail: kakin.lam@abdn.ac.uk (K.K.Lam).

the CBD model in the short-, mid-and long-term forecasting using mortality data of several developed countries in the numerical examples.

Keywords: Demographic modelling; Mortality forecasting; Cohort effects; Time series analysis; Mixed-effects model; CBD model

1 Introduction

Continuous growth in life expectancy has been lasting over the last few decades in many developed countries. This unanticipated increase in lifespan has posed significant challenges to many government sectors and life insurance sectors due to the extra burdens on the health care services and the rapid increase in pension and insurance expenditure. The problem caused by the ageing population is also well-known as the 'longevity risk'. Many demographic researchers have recognised this problem and devoted significant efforts to developing new statistical models for mortality modelling and forecasting. A good statistical model for modelling mortality is always of great importance to incorporate many different factors that help explain the historical mortality patterns and capture their future trends. For example, cohort effects in a statistical mortality model can be considered one of the most important factors but is still underexplored and is missing from the majority of mortality modelling literature, which we aim to discuss and address in this article.

Cohort effects, also known as the year-of-birth effects, are arguably one of the most important and discussed factors that influence mortality experience among groups of individuals born in the same year or generation. Some evidence for the existence of the cohort effects has been successfully spotted, and the developments of the cohort studies can mainly be divided into two different streams. One side relies on the empirical data analysis and the qualitative analysis, such as descriptive and graphical representations, to conclude the existence of cohort

effects on mortality patterns in a population. For example, Willets (2004) discovers that the 'golden generations' cohort who were born between the year 1925 and the year 1945, have experienced exceptionally rapid improvements in mortality rates through examining the average annual mortality improvement rates for males and females in the population of England and Wales. Murphy (2009) and Murphy (2010) further explain this 'golden generations' cohort phenomenon that may be due to those born during and after the Second World War with low fertility and thus facing less competition for resources, better environmental conditions with changing smoking habits and diets between generations. Li et al. (2016) demonstrate the cohort surface across five different countries using graphical presentations with kernel smoothing techniques and conclude that Japan and the UK are the countries with relatively stronger cohort effects than the Netherlands, Spain and the US.

Another side of the cohort studies depends on establishing a new statistical model that offers quantitative approaches to identify the cohort patterns of the observed mortality data. Early attempts can be traced back to the classical age-period-cohort (APC) model in mortality modelling (Holford, 1983). Renshaw & Haberman (2003) extend the well-known Lee-Carter model (Lee & Carter, 1992) by incorporating an age-modulated cohort effects parameter. Cairns et al. (2009) extend their original two-factor Cairns-Blake-Dowd (CBD) model (Cairns et al., 2006) as a three-factor CBD model with cohort parameters. However, the aforementioned statistical mortality models suffer the 'age-period-cohort identification problem', given that the age, period and cohort effects are intertwined¹. Including indicator variables of each level of age, period and cohort respectively in a fixed-effects estimation approach can lead to the perfect collinearity problem, which means that there can be an infinite number of solutions that fit the observed data equally well in the fixed-effects estimation approach (O'Brien, 2014). The common solution to this age-period-cohort identification problem relies on placing pre-specified

¹The age x and period t take values in $\{x_1, \cdots, x_m\}$ and $\{t_1, \cdots, t_n\}$, the cohort index t-x takes values in $\{t_1-x_m, \cdots, t_n-x_1\}$.

constraints on the model coefficients prior to the fitting procedure. However, such pre-specified constraints meanwhile lead to the fitting results of the estimated model parameters substantially depending on the initial constraints chosen (O'Brien, 2017). Readers can refer to Haberman & Renshaw (2011) and Currie (2016) for more comprehensive summaries on these convergence and robustness problems among all these fixed-effects estimation approaches applied to the morality models with the cohort effects parameters.

In this article, we focus on the side of establishing a new statistical mortality model that can extract and provide cohort effects from the observed mortality data for modelling and fore-casting. We propose a novel approach with random cohort effects parameters and age groups dependency structure, which can be seen as a mixed-effects time-series version of the three-factor CBD model with the cohort effects parameters proposed by Cairns et al. (2009). The main contributions of this article are to demonstrate the formulation and parameters estimation of the proposed model with considerations of random cohort effects parameters for mortality modelling and forecasting under a united mixed-effects time-series framework with several desirable advantages over the CBD model.

More will be discussed in detail and the rest of this article is organised as follows. In Section 2, we firstly give a review of the CBD model. In Section 3, we introduce the formulation and the framework of the proposed model for mortality modelling and forecasting. We then illustrate the proposed model with empirical studies of mortality modelling and forecasting with comparisons to the CBD model in terms of the systematic differences and forecasting ability using mortality data of ten different developed countries in Section 4. We lastly conclude this article with discussions and remarks in Section 5.

2 Review of the Cairns-Blake-Dowd (CBD) model

In this section, we define some common actuarial notations used in the CBD model first, and then go through a brief review of the CBD model.

2.1 Actuarial notations and their relationships

In the literature of mortality modelling, there are generally two types of stochastic methods. One type of method models the central mortality rate. The CBD model belongs to the other type of method which models the initial mortality rate. For the sake of notation clarity, we start by defining the notations using a subscript i to denote the number of calendar year t_i for $i = 1, \dots, n$, and a subscript j as the number of age-specific group x_j for $j = 1, \dots, m$ in the CBD model. These notations include as follows:

- D_{x_j,t_i} is the observed number of deaths aged x_j last birthday in a calendar year t_i .
- E_{x_j,t_i}^c is the central exposure to risk aged x_j last birthday in the middle of a calendar year t_i .
- m_{x_j,t_i} is the central mortality rate which reflects the death probability within the range of 0 to 1 for a population died in age x_j last birthday in the middle of a calender year t_i . It is estimated by $m_{x_j,t_i} = D_{x_j,t_i}/E_{x_j,t_i}^c$.
- q_{x_j,t_i} is the initial mortality rate as the one-year death probability between 0 and 1 for a population died in age x_j exactly at time t_i .

The initial mortality rate q_{x_j,t_i} and the central mortality rate m_{x_j,t_i} are typically very close to one another in practice (Dickson et al., 2013). The link between the initial mortality rate and the central mortality rate can be stated, i.e.

$$q_{x_i,t_i} \approx 1 - \exp(-m_{x_i,t_i}),\tag{2.1}$$

where $0 \le q_{x_j,t_i} \le 1$.

2.2 Cairns-Blake-Dowd (CBD) model

The Cairns-Blake-Dowd (CBD) model is one of the most well-known approaches in the mortality modelling literature. Cairns et al. (2009) extend their original two-factor CBD model and propose a three-factor CBD model which incorporates the cohort parameters based on the parsimonious design in their previous version.

We begin by using a subscript i to denote the number of a calendar year t_i for $i=1,\dots,n$, and a subscript j for the number of an age-specific group x_j for $j=1,\dots,m$. The CBD model has the form

$$y_{x_j,t_i} = \operatorname{logit}(q_{x_j,t_i}) = \log\left(\frac{q_{x_j,t_i}}{1 - q_{x_j,t_i}}\right) = \kappa_{t_i}^{(1)} + \kappa_{t_i}^{(2)} \times (x_j - \bar{x}) + \gamma_{t_i - x_j}^{(3)}, \tag{2.2}$$

where y_{x_j,t_i} is the logit of the initial mortality rate at age x_j in a calendar year t_i , $\kappa_{t_i}^{(1)}$ is the general time effects intercept parameter, $\kappa_{t_i}^{(2)}$ is the time effects slope parameter, \bar{x} is the average of the observed mortality data age range, i.e. $\bar{x} = \frac{1}{m} \sum_{j=1}^{m} x_j$, and $\gamma_{t_i-x_j}^{(3)}$ is the cohort effects parameter that provides mortality information on a group of people born in the same calendar year.

The CBD model relies on the linearity of the logit of the initial mortality rate at older ages (age 60 to age 89) by assuming that y_{x_j,t_i} is a response variable of a linear function. It treats $\kappa_{t_i}^{(1)}$ as an intercept term, $\kappa_{t_i}^{(2)}$ as a slope term, and $\gamma_{t_i-x_j}^{(3)}$ as a cohort effects term and assumes all of the terms following stochastic processes for any given calendar year t_i for mortality modelling (Cairns et al., 2009).

2.2.1 Model parameters estimation via the generalised linear modelling approach

Instead of assuming the model error structure is normally distributed and homoscedastic as in many ordinary least squares linear regression approaches, the parameters in the CBD model are estimated based on an alternative approach known as the generalised linear modelling (GLM) approach to calibrate the historical mortality data to the model parameters.

We start with the explanation of the CBD model parameters estimation procedure using the relationship between the initial mortality rate q_{x_j,t_i} and the central mortality rate m_{x_j,t_i} defined in Equation (2.1), and the representation of the CBD model in Equation (2.2). It can be denoted as

$$\log\left(\frac{1 - \exp(-m_{x_j, t_i})}{1 - (1 - \exp(-m_{x_j, t_i}))}\right) = \kappa_{t_i}^{(1)} + \kappa_{t_i}^{(2)} \times (x_j - \bar{x}) + \gamma_{t_i - x_j}^{(3)}.$$
 (2.3)

Rearranging the order of Equation (2.3) with respect to m_{x_i,t_i} , we have

$$m_{x_j,t_i} = \log(1 + \exp(\kappa_{t_i}^{(1)} + \kappa_{t_i}^{(2)} \times (x_j - \bar{x}) + \gamma_{t_i - x_j}^{(3)})).$$

We denote above m_{x_j,t_i} as $m_{x_j,t_i}(\theta_i)$, where $\theta_i = (\kappa_{t_i}^{(1)}, \kappa_{t_i}^{(2)}, \gamma_{t_i-x_j}^{(3)})$ represents the set of the model parameters depending on m_{x_j,t_i} . The CBD model assumes that the number of deaths D_{x_j,t_i} is a random variable from count data following the Poisson distribution, i.e.

$$D_{x_i,t_i} \sim \text{Poisson}(E_{x_i,t_i}^c \times m_{x_i,t_i}(\theta_i)).$$

We can thus state the log-likelihood function of heta conditional on D and E^c across all agespecific groups and calender years as

$$\mathcal{L}(\boldsymbol{\theta}|\boldsymbol{D}, \boldsymbol{E^c}) = \sum_{i=1}^{n} \sum_{j=1}^{m} D_{x_j, t_i} \times \log(E_{x_j, t_i}^c \times m_{x_j, t_i}(\theta_i)) - E_{x_j, t_i}^c \times m_{x_j, t_i}(\theta_i) - \log(D_{x_j, t_i}!), \quad (2.4)$$

where θ is the full set of the model parameters matrix, D is the observed number of deaths matrix across all age-specific groups and calender years, and E^c is the central exposure matrix across all age-specific groups and calender years.

However, the full set of the model parameters cannot simply be calibrated by maximising the above log-likelihood function to have a closed form solution as the log-likelihood function follows the Poisson distribution. The model itself also suffers model identification problems, in which the model parameters are over-parametrised in Equation (2.2) since there can be two or more possible model structures. For example, we can see that they are invariant to the following transformation

$$\left(\kappa_{t_i}^{(1)}, \kappa_{t_i}^{(2)}, \gamma_{t_i - x_j}^{(3)}\right) \mapsto \left(\kappa_{t_i}^{(1)} + \phi_1 + \phi_2 \times (t_i - \bar{x}), \kappa_{t_i}^{(2)} - \phi_2, \gamma_{t_i - x_j}^{(3)} - \phi_1 - \phi_2 \times (t_i - x_j)\right),$$

where ϕ_1 and ϕ_2 are any non-zero constants.

Cairns et al. (2009) amend this identification problem by switching the cohort effects parameter from $\gamma_{t_i-x_j}^{(3)}$ to $\tilde{\gamma}_{t_i-x_j}^{(3)} = \phi_1 + \phi_2 \times (t_i-x_j) + \gamma_{t_i-x_j}^{(3)}$ and imposing the following constraints on the cohort parameter $\gamma_{t_i-x_j}^{(3)}$ throughout the iterative optimisation process for the log-likelihood function in Equation (2.4), such that

$$\sum_{\substack{(t_i - x_j) \in C}} \gamma_{t_i - x_j}^{(3)} = 0,$$

$$\sum_{\substack{(t_i - x_j) \in C}} (t_i - x_j) \times \gamma_{t_i - x_j}^{(3)} = 0,$$

where C is the set of cohort years of birth $(t_i - x_j)$ included in the analysis. Cairns et al. (2009) explain the choice of the above constraints is analogous to fitting a latent linear function of $\phi_1 + \phi_2 \times (t_i - x_j)$ to $\gamma_{t_i - x_j}^{(3)}$ implicitly, so that the constraints ensure $\hat{\phi}_1 = 0$ and $\hat{\phi}_2 = 0$, and the fitted $\hat{\gamma}_{t_i - x_j}^{(3)}$ will fluctuate around zero and has no discernible linear trend as a standard normal random variable. Cairns et al. (2009), Haberman & Renshaw (2011) and Currie (2016) provide further discussions on these identifiability and parameter fitting issues for the three-factor CBD model.

2.2.2 Out-of-sample forecasts of the mortality odds in the CBD model

For the out-of-sample forecasts of the initial mortality rate, Cairns et al. (2006) assume that the fitted $\hat{\kappa}_{t_i}^{(1)}$ and $\hat{\kappa}_{t_i}^{(2)}$ follow a bivariate random walk with drift which can be described by defining $\hat{\beta}_{t_i} = \begin{pmatrix} \hat{\kappa}_{t_i}^{(1)} \\ \hat{\kappa}_{t_i}^{(2)} \end{pmatrix}$, then we have

$$\hat{oldsymbol{eta}}_{t_i} = \hat{oldsymbol{eta}}_{t_{i-1}} + oldsymbol{d} + oldsymbol{K} oldsymbol{Z}_{t_i},$$

where d is a 2×1 vector of the drift factors and Z_{t_i} is a 2×1 vector of bivariate normally distributed random variables, i.e. $Z_{t_i} \sim \mathcal{N}_{2\times 1}(\mathbf{0}, \mathbf{I})$. Let \mathbf{V} be a variance-covariance matrix of $\hat{\kappa}_{t_i}^{(1)}$ and $\hat{\kappa}_{t_i}^{(2)}$. Without loss of generality, \mathbf{K} is restricted to be an upper triangular matrix by Cholesky decomposition where $\mathbf{V} = \mathbf{K}^T \mathbf{K}$. Denoting Δ as a first-difference operator, such that $\Delta \hat{\kappa}_{t_i}^{(l)} = \hat{\kappa}_{t_i}^{(l)} - \hat{\kappa}_{t_{i-1}}^{(l)}$ for l = 1, 2, we can estimate \mathbf{d} and \mathbf{V} as

$$\hat{m{d}} = egin{pmatrix} \mathbb{E}(\Delta \hat{\kappa}_{t_i}^{(1)}) \ \mathbb{E}(\Delta \hat{\kappa}_{t_i}^{(2)}) \end{pmatrix},$$

and let $\hat{\sigma}_{lk} = \mathbb{E}[(\Delta \hat{\kappa}_{t_i}^{(l)} - \mathbb{E}(\Delta \hat{\kappa}_{t_i}^{(l)}))^T (\Delta \hat{\kappa}_{t_i}^{(k)} - \mathbb{E}(\Delta \hat{\kappa}_{t_i}^{(k)}))]$ for l, k = 1, 2,

$$\hat{m{V}} = egin{pmatrix} \hat{\sigma}_{11} & \hat{\sigma}_{12} \ \hat{\sigma}_{21} & \hat{\sigma}_{22} \end{pmatrix}.$$

By Cholesky decomposition of \hat{V} , we have

$$\hat{\boldsymbol{V}} = \hat{\boldsymbol{K}}^T \hat{\boldsymbol{K}}.$$

The h-step ahead extrapolation of $\hat{oldsymbol{eta}}_{t_i}$ is then

$$\hat{oldsymbol{eta}}_{t_{i+h}} = \hat{oldsymbol{eta}}_{t_{i+h-1}} + \hat{oldsymbol{d}},$$

and the variance of the h-step ahead extrapolation of $\hat{\beta}_{t_i}$ is

$$\operatorname{Var}(\boldsymbol{\beta}_{t_{i+h}}) = h \times \hat{\boldsymbol{V}}.$$

The cohort effects parameter $\hat{\gamma}_{t_i-x_j}^{(3)}$ is assumed to follow a univariate random walk with drift (Haberman & Renshaw, 2011), hence the h-step ahead extrapolation of $\hat{\gamma}_{t_i-x_j}^{(3)}$ is

$$\hat{\gamma}_{t_{i+h}-x_{i}}^{(3)} = \hat{\gamma}_{t_{i+h-1}-x_{i}}^{(3)} + \hat{\mu},$$

where $\hat{\mu} = \mathbb{E}(\Delta \hat{\gamma}_{t_i - x_j}^{(3)})$.

Combining all the extrapolated model parameters in the CBD model, the h-step ahead out-of-sample forecast of y_{x_i,t_i} is

$$\hat{y}_{x_j,t_{i+h}} = \hat{\kappa}_{t_{i+h}}^{(1)} + \hat{\kappa}_{t_{i+h}}^{(2)} \times (x_j - \bar{x}) + \hat{\gamma}_{t_{i+h}-x_j}^{(3)}.$$

3 Methodology

3.1 Mixed-effects time-series model with age groups dependency and random cohort effects parameters

In this section, we introduce the proposed mixed-effects time-series model with age groups dependency and random cohort effects parameters.

Let our observed mortality dataset be $\{t_i, x_j, y_{x_j, t_i}\}$ for i = 1, ..., n and j = 1, ..., m, where n is the total number of observed calendar years, m is the maximum number of agespecific groups of interest, y_{x_j, t_i} is the logit of the initial mortality rate for age x_j in a calendar year t_i . The proposed mixed-effects time-series model is

$$y_{x_j,t_i} = \operatorname{logit}(q_{x_j,t_i}) = \operatorname{log}\left(\frac{q_{x_j,t_i}}{1 - q_{x_i,t_i}}\right) = f_{x_j}(t_i - \overline{t}) + \epsilon_{x_j,t_i}, \quad \epsilon_{x_j,t_i} \sim \mathcal{N}(0,\sigma^2),$$

where $f_{x_j}(t_i - \bar{t})$ is an underlying function which needs to be estimated for a given age x_j , \bar{t} is the average of the observed calendar years, i.e. $\bar{t} = \frac{1}{n} \sum_{i=1}^{n} t_i$, and $\{\epsilon_{x_j,t_i}\}_{i,j=1}^{n,m}$ allow the observation error varying among the different age groups and the calendar years based on the assumption of i.i.d. normally distributed random variables with mean 0 and constant variance σ^2 .

The underlying function $f_{x_j}(t_i - \bar{t})$ in the proposed model under the mixed-effects structure is further specified as

$$f_{x_j}(t_i - \bar{t}) = \mu(t_i - \bar{t}) + \eta_{x_j}(t_i - \bar{t}),$$

where $\mu(t_i - \bar{t})$ is a general linear mean function across all age groups $\{x_j\}_{j=1}^m$, i.e.

$$\mu(t_i - \bar{t}) = \beta^{(1)} + \beta^{(2)} \times (t_i - \bar{t}),$$

with $\beta^{(1)}$ is the fixed-effects intercept parameter and $\beta^{(2)}$ is the fixed-effects slope parameter multiplying the input $(t_i - \bar{t})$.

Meanwhile, $\eta_{x_j}(t_i - \bar{t})$ is the age-specific deviation function from the general linear mean function across all age groups, which is designed to be a function with the following components

$$\eta_{x_j}(t_i - \bar{t}) = f_{x_j}(t_i - \bar{t}) - \mu(t_i - \bar{t}) = \gamma_{x_j}^{(1)} + \gamma_{x_j}^{(2)} \times (t_i - \bar{t}) + \gamma_{t_i - x_j}^{(3)}, \tag{3.1}$$

where we assume that $\{\gamma_{x_j}^{(1)}\}_{j=1}^m$ are the correlated age-specific random effects intercept parameters following a prior distribution $(\gamma_{x_1}^{(1)},\ldots,\gamma_{x_m}^{(1)})^T\sim\mathcal{N}(\mathbf{0},\boldsymbol{K}^{(1)}),$ $\{\gamma_{x_j}^{(2)}\}_{j=1}^m$ are the correlated age-specific random effects slope parameters following a prior distribution $(\gamma_{x_1}^{(2)},\ldots,\gamma_{x_m}^{(2)})^T\sim\mathcal{N}(\mathbf{0},\boldsymbol{K}^{(2)}),$ and $\{\gamma_{t_i-x_j}^{(3)}\}_{t_1-x_m}^{t_n-x_1}$ are the correlated age-specific random effects cohort parameters following a prior distribution $(\gamma_{t_1-x_m}^{(3)},\ldots,\gamma_{t_n-x_1}^{(3)})^T\sim\mathcal{N}(\mathbf{0},\boldsymbol{K}^{(3)})^2.$

With all the designed components mentioned above, we can state the full form of the proposed model as

$$y_{x_j,t_i} = \beta^{(1)} + \beta^{(2)} \times (t_i - \bar{t}) + \gamma_{x_j}^{(1)} + \gamma_{x_j}^{(2)} \times (t_i - \bar{t}) + \gamma_{t_i - x_j}^{(3)} + \epsilon_{x_j,t_i}.$$
(3.2)

Alternatively, we can group $\kappa_{x_j}^{(1)} = \beta^{(1)} + \gamma_{x_j}^{(1)}$ and $\kappa_{x_j}^{(2)} = \beta^{(2)} + \gamma_{x_j}^{(2)}$ for the simplicity of notation, and the proposed model is thus

$$y_{x_j,t_i} = \kappa_{x_j}^{(1)} + \kappa_{x_j}^{(2)} \times (t_i - \bar{t}) + \gamma_{t_i - x_j}^{(3)} + \epsilon_{x_j,t_i}.$$

3.2 Formulation and parameters estimation of the proposed model

In this section, we begin by describing the formulation of the proposed model and explain the procedure of the model parameters estimation.

3.2.1 Model formulation

Letting $\boldsymbol{Y}_{x_j} = [y_{x_j,t_1}, y_{x_j,t_2}, \dots, y_{x_j,t_n}]^T$, $\boldsymbol{T}_{x_j} = [(t_1 - \bar{t}), (t_2 - \bar{t}), \dots, (t_n - \bar{t})]^T$ and $\boldsymbol{\varepsilon}_{x_j} = [\varepsilon_{x_j,t_1}, \varepsilon_{x_j,t_2}, \dots, \varepsilon_{x_j,t_n}]^T$, we can denote Equation (3.2) in matrix form as

$$Y = T\beta + Z^{(1)}\gamma_x^{(1)} + Z^{(2)}\gamma_x^{(2)} + Z^{(3)}\gamma_{t-x}^{(3)} + \epsilon, \quad \epsilon \sim N(0, \sigma^2 I),$$
 (3.3)

²Without any loss of completeness, the covariance structures of all the random effects components $\gamma_{x_j}^{(1)}$, $\gamma_{x_j}^{(2)}$ and $\gamma_{t_i-x_j}^{(3)}$ will be discussed in Section 3.2.

where

$$oldsymbol{Y} = egin{bmatrix} oldsymbol{Y}_{x_1} \ oldsymbol{Y}_{x_2} \ dots \ oldsymbol{Y}_{x_m} \end{bmatrix} \in \mathbb{R}^{nm imes 1}, oldsymbol{T} = egin{bmatrix} oldsymbol{1}_{n imes 1} & oldsymbol{T}_{x_2} \ dots & dots \ oldsymbol{1}_{n imes 1} & oldsymbol{T}_{x_m} \end{bmatrix} \in \mathbb{R}^{nm imes 2}, oldsymbol{eta} = egin{bmatrix} eta^{(1)} \ eta^{(2)} \end{bmatrix} \in \mathbb{R}^{2 imes 1},$$

$$\boldsymbol{Z}^{(1)} = \begin{bmatrix} \mathbf{1}_{n \times 1} & 0 & \dots & 0 & 0 \\ 0 & \mathbf{1}_{n \times 1} & \dots & 0 & 0 \\ \vdots & \vdots & \ddots & \vdots & \vdots \\ 0 & 0 & \dots & 0 & \mathbf{1}_{n \times 1} \end{bmatrix} \in \mathbb{R}^{nm \times m}, \boldsymbol{\gamma}_{\boldsymbol{x}}^{(1)} = \begin{bmatrix} \boldsymbol{\gamma}_{x_1}^{(1)} \\ \boldsymbol{\gamma}_{x_2}^{(1)} \\ \vdots \\ \boldsymbol{\gamma}_{x_m}^{(1)} \end{bmatrix} \in \mathbb{R}^{m \times 1},$$

$$\boldsymbol{Z}^{(2)} = \begin{bmatrix} \boldsymbol{T}_{x_1} & 0 & \dots & 0 & 0 \\ 0 & \boldsymbol{T}_{x_2} & \dots & 0 & 0 \\ \vdots & \vdots & \ddots & \vdots & \vdots \\ 0 & 0 & \dots & 0 & \boldsymbol{T}_{x_m} \end{bmatrix} \in \mathbb{R}^{nm \times m}, \boldsymbol{\gamma}_{\boldsymbol{x}}^{(2)} = \begin{bmatrix} \boldsymbol{\gamma}_{x_1}^{(2)} \\ \boldsymbol{\gamma}_{x_2}^{(2)} \\ \vdots \\ \boldsymbol{\gamma}_{x_m}^{(2)} \end{bmatrix} \in \mathbb{R}^{m \times 1},$$

$$\mathbf{Z}^{(3)} = \begin{bmatrix} t_1 - x_m & t_2 - x_m & \dots & t_n - x_m & t_n - x_{m-1} & \dots & t_n - x_1 \\ t_2 - x_1 & 0 & 0 & \dots & 0 & 0 & \dots & 0 \\ \vdots & \vdots & \vdots & \ddots & \vdots & \vdots & \ddots & \vdots \\ t_n - x_1 & 0 & 0 & \dots & 0 & 0 & \dots & 1 \\ t_1 - x_2 & 0 & 0 & \dots & 0 & 0 & \dots & 0 \\ t_2 - x_2 & 0 & 0 & \dots & 0 & 0 & \dots & 0 \\ \vdots & \vdots & \vdots & \ddots & \vdots & \vdots & \ddots & \vdots \\ t_n - x_2 & 0 & 0 & \dots & 0 & 0 & \dots & 0 \\ \vdots & \vdots & \vdots & \ddots & \vdots & \vdots & \ddots & \vdots \\ t_{1-x_{m-1}} & 0 & 0 & \dots & 0 & 0 & \dots & 0 \\ t_{2-x_{m-1}} & 0 & 0 & \dots & 0 & 0 & \dots & 0 \\ \vdots & \vdots & \vdots & \ddots & \vdots & \vdots & \ddots & \vdots \\ t_{n-x_{m-1}} & 0 & 0 & \dots & 0 & 1 & \dots & 0 \\ t_{1-x_m} & 1 & 0 & \dots & 0 & 0 & \dots & 0 \\ t_{2-x_m} & 0 & 1 & \dots & 0 & 0 & \dots & 0 \\ \vdots & \vdots & \vdots & \ddots & \vdots & \vdots & \ddots & \vdots \\ t_{n-x_m} & 0 & 1 & \dots & 0 & 0 & \dots & 0 \\ \vdots & \vdots & \vdots & \ddots & \vdots & \vdots & \ddots & \vdots \\ t_{n-x_m} & 0 & 0 & \dots & 1 & 0 & \dots & 0 \end{bmatrix}$$

year t / age x	x = 1	x=2	x = 3
t = 1	$\gamma_0^{(3)}$	$\gamma_{-1}^{(3)}$	$\gamma_{-2}^{(3)}$
t=2	$\gamma_1^{(3)}$	$\gamma_0^{(3)}$	$\gamma_{-1}^{(3)}$

Table 3.1: Values of the cohort effects parameters $\gamma_{t-x}^{(3)}$ in a matrix of cells (t,x).

$$\boldsymbol{\gamma_{t-x}^{(3)}} = \begin{bmatrix} \gamma_{t_1-x_m}^{(3)} \\ \gamma_{t_2-x_m}^{(3)} \\ \vdots \\ \gamma_{t_n-x_m}^{(3)} \\ \gamma_{t_n-x_{m-1}}^{(3)} \\ \vdots \\ \gamma_{t_n-x_1}^{(3)} \end{bmatrix} \in \mathbb{R}^{(n+m-1)\times 1}, \text{ and } \boldsymbol{\epsilon} = \begin{bmatrix} \boldsymbol{\epsilon}_{x_1} \\ \boldsymbol{\epsilon}_{x_2} \\ \vdots \\ \boldsymbol{\epsilon}_{x_m} \end{bmatrix} \in \mathbb{R}^{nm\times 1}.$$

In aid of explaining the above full matrix representation of the proposed model, here we consider a smaller matrix of cells where the row and column of the matrix directly correspond to year t and age x without the use of script for illustration purposes. The cohort effects parameter $\gamma_{t-x}^{(3)}$ is indexed by the year-of-birth and its corresponding value on each cell is displayed in Table 3.1 for the cohort effects. We can see that the index values of $\gamma_{t-x}^{(3)}$ are the same in the 'cohort direction', which are on the cells (x,t), (x+1,t+1) and so on. The total number of cohort effects parameters is equal to the number of rows plus the number of columns minus one, which is four in our illustration here. The proposed model with the smaller size of matrix cells can be expressed as

$$\begin{bmatrix} y_{x_1,t_1} \\ y_{x_1,t_2} \\ y_{x_2,t_1} \\ y_{x_2,t_2} \\ y_{x_3,t_1} \\ y_{x_3,t_2} \end{bmatrix} = \begin{bmatrix} 1 & t_1 \\ 1 & t_2 \\ 1 & t_1 \\ 1 & t_2 \end{bmatrix} \begin{bmatrix} \beta^{(1)} \\ \beta^{(2)} \end{bmatrix} + \begin{bmatrix} 1 & 0 & 0 \\ 1 & 0 & 0 \\ 0 & 1 & 0 \\ 0 & 0 & 1 \\ 0 & 0 & 1 \end{bmatrix} \begin{bmatrix} \gamma^{(1)}_{x_1} \\ \gamma^{(1)}_{x_2} \\ \gamma^{(1)}_{x_3} \\ \gamma^{(1)}_{x_3} \end{bmatrix} + \begin{bmatrix} t_1 & 0 & 0 \\ t_2 & 0 & 0 \\ 0 & t_1 & 0 \\ 0 & 0 & t_1 \\ 0 & 0 & t_2 \end{bmatrix} \begin{bmatrix} \gamma^{(2)}_{x_1} \\ \gamma^{(2)}_{x_2} \\ \gamma^{(2)}_{x_3} \end{bmatrix} + \begin{bmatrix} 0 & 0 & 1 & 0 \\ 0 & 0 & 0 & 1 \\ 0 & 1 & 0 & 0 \\ 0 & 0 & 1 & 0 \\ 0 & 0 & 0 & 1 \\ 0 & 0 & 0 & 0 \end{bmatrix} \begin{bmatrix} \gamma^{(3)}_{-2} \\ \gamma^{(3)}_{-1} \\ \gamma^{(3)}_{0} \\ \gamma^{(3)}_{1} \end{bmatrix} + \begin{bmatrix} \epsilon_{x_1,t_1} \\ \epsilon_{x_1,t_2} \\ \epsilon_{x_2,t_1} \\ \epsilon_{x_3,t_1} \\ \epsilon_{x_3,t_2} \end{bmatrix} .$$

For the stochastic components in the proposed model, we assume that the prior distributions of $\gamma_{x}^{(1)} \sim \mathcal{N}(\mathbf{0}, \mathbf{K}^{(1)}), \ \gamma_{x}^{(2)} \sim \mathcal{N}(\mathbf{0}, \mathbf{K}^{(2)})$ and $\gamma_{t-x}^{(3)} \sim \mathcal{N}(\mathbf{0}, \mathbf{K}^{(3)})$. $\mathbf{K}^{(1)}$ and $\mathbf{K}^{(2)}$ are both $m \times m$ squared exponential covariance matrices which are used to model the dependence

structure among different age groups. They have the following form, for i = 1, 2, i.e.

$$\boldsymbol{K}^{(i)} = h_i^2 \exp \left(- \begin{bmatrix} \frac{(x_1 - x_1)^2}{2l_i} & \frac{(x_1 - x_2)^2}{2l_i} & \dots & \frac{(x_1 - x_m)^2}{2l_i} \\ \frac{(x_2 - x_1)^2}{2l_i} & \frac{(x_2 - x_2)^2}{2l_i} & \dots & \frac{(x_2 - x_m)^2}{2l_i} \\ \vdots & \vdots & \ddots & \vdots \\ \frac{(x_m - x_1)^2}{2l_i} & \frac{(x_m - x_2)^2}{2l_i} & \dots & \frac{(x_m - x_m)^2}{2l_i} \end{bmatrix} \right),$$

where h_i is the response-scale amplitude parameter determining the variation of function values, and l_i is the characteristic length-scale parameter that gives smooth variations in a covariate-scale and controls how close the varying age groups should correlate.

 $\boldsymbol{K}^{(3)}$ is another $(n+m-1)\times(n+m-1)$ squared exponential covariance matrix for $\boldsymbol{\gamma_{t-x}^{(3)}}$ modelling the dependence structure among different groups of people born in the same year with the following form

$$\boldsymbol{K}^{(3)} = c^{2} \exp \left(- \begin{bmatrix} \frac{((t_{1} - x_{m}) - (t_{1} - x_{m}))^{2}}{2s} & \frac{((t_{1} - x_{m}) - (t_{2} - x_{m}))^{2}}{2s} & \cdots & \frac{((t_{1} - x_{m}) - (t_{n} - x_{1}))^{2}}{2s} \\ \frac{((t_{2} - x_{m}) - (t_{1} - x_{m}))^{2}}{2s} & \frac{((t_{2} - x_{m}) - (t_{2} - x_{m}))^{2}}{2s} & \cdots & \frac{((t_{2} - x_{m}) - (t_{n} - x_{1}))^{2}}{2s} \\ \vdots & \vdots & \ddots & \vdots \\ \frac{((t_{n} - x_{1}) - (t_{1} - x_{m}))^{2}}{2s} & \frac{((t_{n} - x_{1}) - (t_{2} - x_{m}))^{2}}{2s} & \cdots & \frac{((t_{n} - x_{1}) - (t_{n} - x_{1}))^{2}}{2s} \end{bmatrix} \right).$$

where c is the response-scale amplitude parameter that determines the variation of function values, and s is the characteristic length-scale parameter that gives smooth variations in a covariate-scale and controls how close the different groups of people born in the same year should correlate.

The main justification of choosing the squared exponential covariance matrices here for all the stochastic components is to reflect the dependencies among different age groups properly as we assume that people who are closer in age groups or birth year would tend to have more similarities in their mortality patterns than those who are in distant age ranges or were born in a different generation.

With the prior distribution assumptions among all the random effects components, Equation (3.3) can be restated as a multivariate normal distribution among all its random effects

components, i.e.

$$Y = T\beta + Z^{(1)}\gamma_x^{(1)} + Z^{(2)}\gamma_x^{(2)} + Z^{(3)}\gamma_{t-x}^{(3)} + \epsilon,$$
(3.4)

where

$$\begin{bmatrix} \boldsymbol{\gamma}_{x}^{(1)} \\ \boldsymbol{\gamma}_{x}^{(2)} \\ \boldsymbol{\gamma}_{t-x}^{(3)} \\ \boldsymbol{\varepsilon} \end{bmatrix} \sim \mathcal{N} \Bigg(\begin{bmatrix} \mathbf{0} \\ \mathbf{0} \\ \mathbf{0} \\ \mathbf{0} \end{bmatrix}, \begin{bmatrix} \boldsymbol{K}^{(1)} & \mathbf{0} & \mathbf{0} & \mathbf{0} \\ \mathbf{0} & \boldsymbol{K}^{(2)} & \mathbf{0} & \mathbf{0} \\ \mathbf{0} & \mathbf{0} & \boldsymbol{K}^{(3)} & \mathbf{0} \\ \mathbf{0} & \mathbf{0} & \mathbf{0} & \sigma^{2} \boldsymbol{I} \end{bmatrix} \Bigg).$$

3.2.2 Model parameters inference

With the model formulation specified in the previous section, we can infer the model parameters by the Bayesian paradigm. The probability distribution of \mathbf{Y} in Equation (3.4) is given by $\mathcal{N}(T\boldsymbol{\beta}, \mathbf{V}(\boldsymbol{\theta}))$ where $\mathbf{V}(\boldsymbol{\theta}) = \mathbf{Z}^{(1)} \mathbf{K}^{(1)} \mathbf{Z}^{(1)^T} + \mathbf{Z}^{(2)} \mathbf{K}^{(2)} \mathbf{Z}^{(2)^T} + \mathbf{Z}^{(3)} \mathbf{K}^{(3)} \mathbf{Z}^{(3)^T} + \sigma^2 \mathbf{I}$. $\mathbf{V}(\boldsymbol{\theta})$ is the $nm \times nm$ variance-covariance matrix parametrised by the (hyper-) parameters $\boldsymbol{\theta} = [h^{(1)}, l^{(1)}, h^{(2)}, l^{(2)}, c, s]^T$ involved in its components covariance matrices $\mathbf{K}^{(1)}, \mathbf{K}^{(2)}, \mathbf{K}^{(3)}$ and the random error variance σ^2 . Hence the log-likelihood function of $\boldsymbol{\beta}$, the parameters of the variance-covariance matrix $\boldsymbol{\theta}$ and the random error variance σ^2 is

$$\mathcal{L}(\boldsymbol{\beta}, \boldsymbol{\theta}, \sigma^2) = -\frac{1}{2} \log |\boldsymbol{V}(\boldsymbol{\theta})| - \frac{1}{2} (\boldsymbol{Y} - \boldsymbol{T}\boldsymbol{\beta})^T \boldsymbol{V}(\boldsymbol{\theta})^{-1} (\boldsymbol{Y} - \boldsymbol{T}\boldsymbol{\beta}) - \frac{nm}{2} \log(2\pi), \quad (3.5)$$

where $|\cdot|$ is the determinant of a matrix.

Given that there is no analytical closed-form solution to this maximisation problem, we need to resort to some standard gradient-based numerical optimisation techniques, such as the Newton-Raphson method or the Conjugate Gradient method, to maximise the log-likelihood function $\mathcal{L}(\boldsymbol{\beta}, \boldsymbol{\theta}, \sigma^2)$ in Equation (3.5) for obtaining the optimal estimates of the model parameters.

To set the form of the model parameters appropriate for the iterative process of the gradient-based optimisation method, we seek to differentiate the log-likelihood function $\mathcal{L}(\boldsymbol{\beta}, \boldsymbol{\theta}, \sigma^2)$ with

respect to its elements β , θ , and σ^2 . This yields the following partial derivatives

$$\frac{\partial \mathcal{L}(\boldsymbol{\beta}, \boldsymbol{\theta}, \sigma^2)}{\partial \boldsymbol{\beta}} = -(\boldsymbol{T}^T \boldsymbol{V}(\boldsymbol{\theta})^{-1} \boldsymbol{T} \boldsymbol{\beta} - \boldsymbol{T}^T \boldsymbol{V}(\boldsymbol{\theta})^{-1} \boldsymbol{Y}), \tag{3.6}$$

$$\frac{\partial \mathcal{L}(\boldsymbol{\beta}, \boldsymbol{\theta}, \sigma^2)}{\partial \theta_i} = -\frac{1}{2} \left\{ \operatorname{tr} \left(\boldsymbol{V}(\boldsymbol{\theta})^{-1} \frac{\partial \boldsymbol{V}(\boldsymbol{\theta})}{\partial \theta_i} \right) + (\boldsymbol{Y} - \boldsymbol{T}\boldsymbol{\beta})^T \left(\boldsymbol{V}(\boldsymbol{\theta})^{-1} \frac{\partial \boldsymbol{V}(\boldsymbol{\theta})}{\partial \theta_i} \boldsymbol{V}(\boldsymbol{\theta})^{-1} \right) (\boldsymbol{Y} - \boldsymbol{T}\boldsymbol{\beta}) \right\},$$

$$\frac{\partial \mathcal{L}(\boldsymbol{\beta}, \boldsymbol{\theta}, \sigma^2)}{\partial \sigma^2} = -\frac{1}{2} \left\{ \operatorname{tr} (\boldsymbol{V}(\boldsymbol{\theta})^{-1}) + (\boldsymbol{Y} - \boldsymbol{T}\boldsymbol{\beta})^T (\boldsymbol{V}(\boldsymbol{\theta})^{-1} \boldsymbol{V}(\boldsymbol{\theta})^{-1}) (\boldsymbol{Y} - \boldsymbol{T}\boldsymbol{\beta}) \right\},$$

where θ_i is a generic notation of the ith element of parameters in the vector $\boldsymbol{\theta}$.

Setting Equation (3.6) equal to zero and solving it give us the closed-form maximum likelihood estimator $\hat{\beta}$, i.e.

$$\hat{\boldsymbol{\beta}} = (\boldsymbol{T}^T \boldsymbol{V}(\boldsymbol{\theta})^{-1} \boldsymbol{T})^{-1} \boldsymbol{T}^T \boldsymbol{V}(\boldsymbol{\theta})^{-1} \boldsymbol{Y}.$$
 (3.7)

The typical iterative procedure in the gradient-based optimiser for estimating β , θ and σ^2 with the above partial derivatives involves the following four steps:

- 1. Assign initial values to $\hat{\boldsymbol{\theta}}_{(1)} = [\hat{h}_{(1)}^{(1)}, \hat{l}_{(1)}^{(1)}, \hat{h}_{(1)}^{(2)}, \hat{l}_{(1)}^{(2)}, \hat{c}_{(1)}, \hat{s}_{(1)}]^T$ and $\hat{\sigma}_{(1)}^2$.
- 2. Substitute $\hat{\theta}_{(k)}$ and $\hat{\sigma}_{(k)}^2$ to solve for $\hat{\beta}_{(k)}$ in Equation (3.7) and calculate the value of the following log-likelihood function in each k^{th} step iteration:

$$\mathcal{L}(\hat{\boldsymbol{\beta}}_{(k)}, \hat{\boldsymbol{\theta}}_{(k)}, \hat{\sigma}_{(k)}^2) = -\frac{1}{2} \log |\boldsymbol{V}(\hat{\boldsymbol{\theta}}_{(k)})| - \frac{1}{2} (\boldsymbol{Y} - \boldsymbol{T}\hat{\boldsymbol{\beta}}_{(k)})^T \boldsymbol{V}(\hat{\boldsymbol{\theta}}_{(k)})^{-1} (\boldsymbol{Y} - \boldsymbol{T}\hat{\boldsymbol{\beta}}_{(k)}) - \frac{nm}{2} \log(2\pi).$$

- 3. Update $\hat{\theta}_{i,(k+1)} = \hat{\theta}_{i,(k)} + \frac{\partial \mathcal{L}(\hat{\boldsymbol{\beta}}_{(k)},\hat{\boldsymbol{\theta}}_{(k)},\hat{\sigma}^2_{(k)})/\partial \hat{\theta}_{i,(k)}}{\partial^2 \mathcal{L}(\hat{\boldsymbol{\beta}}_{(k)},\hat{\boldsymbol{\theta}}_{(k)},\hat{\sigma}^2_{(k)})/\partial^2 \hat{\theta}_{i,(k)}}$ and $\hat{\sigma}^2_{(k+1)} = \hat{\sigma}^2_{(k)} + \frac{\partial \mathcal{L}(\hat{\boldsymbol{\beta}}_{(k)},\hat{\boldsymbol{\theta}}_{(k)},\hat{\sigma}^2_{(k)})/\partial^2 \hat{\sigma}^2_{(k)}}{\partial^2 \mathcal{L}(\hat{\boldsymbol{\beta}}_{(k)},\hat{\boldsymbol{\theta}}_{(k)},\hat{\sigma}^2_{(k)})/\partial^2 \hat{\sigma}^2_{(k)}}$ based on the gradient ascent criteria.
- 4. Repeat Step 2 and Step 3 until the above log-likelihood function converges ³.

³The performances of the gradient-based optimisation approaches may depend on the initial values supplied. Several optimisations running can be applied with different initial values may be necessary if no prior knowledge about the function to optimise.

Once the estimated $\hat{\boldsymbol{\theta}}_{(p)}$, $\hat{\sigma}_{(p)}^2$ and $\boldsymbol{V}(\hat{\boldsymbol{\theta}}_{(p)})$ are obtained in the p^{th} step iteration where the log-likelihood function converges, we have

$$egin{bmatrix} m{Y} \ m{\gamma_{x}^{(1)}} \ m{\gamma_{x}^{(2)}} \ m{\gamma_{t-x}^{(3)}} \end{bmatrix} \sim \mathcal{N} egin{bmatrix} m{T}\hat{m{eta}}_{(p)} \ m{0} \ m{0} \end{bmatrix}, egin{bmatrix} m{V}(\hat{m{ heta}}_{(p)}) & m{Z}^{(1)}\hat{m{K}}^{(1)} & m{Z}^{(2)}\hat{m{K}}^{(2)} & m{Z}^{(3)}\hat{m{K}}^{(3)} \ m{\hat{K}}^{(1)}m{Z}^{(1)^T} & \hat{m{K}}^{(1)} & m{0} & m{0} \ \hat{m{K}}^{(2)} & m{Z}^{(2)^T} & m{0} & \hat{m{K}}^{(2)} & m{0} \ \hat{m{K}}^{(3)} & m{Z}^{(3)} \end{bmatrix} m{N}, \end{array}$$

and the conditional distributions of $\gamma_x^{(1)}$, $\gamma_x^{(2)}$, $\gamma_{t-x}^{(3)}$ given Y follow the multivariate Gaussian distribution, which are $\gamma_x^{(1)}|Y \sim \mathcal{N}(\hat{\gamma}_x^{(1)}, \text{Var}(\gamma_x^{(1)}))$, $\gamma_x^{(2)}|Y \sim \mathcal{N}(\hat{\gamma}_x^{(2)}, \text{Var}(\gamma_x^{(2)}))$ and $\gamma_{t-x}^{(3)}|Y \sim \mathcal{N}(\hat{\gamma}_{t-x}^{(3)}, \text{Var}(\gamma_{t-x}^{(3)}))$, where

$$\hat{\boldsymbol{\gamma}}_{x}^{(1)} = \hat{\boldsymbol{K}}^{(1)} \boldsymbol{Z}^{(1)^{T}} \boldsymbol{V} (\hat{\boldsymbol{\theta}}_{(p)})^{-1} (\boldsymbol{Y} - \boldsymbol{T} \hat{\boldsymbol{\beta}}_{(p)}), \tag{3.8}$$

$$\operatorname{Var}(\boldsymbol{\gamma}_{x}^{(1)}) = \hat{\boldsymbol{K}}^{(1)} - [\hat{\boldsymbol{K}}^{(1)} \boldsymbol{Z}^{(1)^{T}} \boldsymbol{V} (\hat{\boldsymbol{\theta}}_{(p)})^{-1} \boldsymbol{Z}^{(1)} \hat{\boldsymbol{K}}^{(1)}],$$

$$\hat{\boldsymbol{\gamma}}_{x}^{(2)} = \hat{\boldsymbol{K}}^{(2)} \boldsymbol{Z}^{(2)^{T}} \boldsymbol{V} (\hat{\boldsymbol{\theta}}_{(p)})^{-1} (\boldsymbol{Y} - \boldsymbol{T} \hat{\boldsymbol{\beta}}_{(p)}), \tag{3.9}$$

$$\operatorname{Var}(\boldsymbol{\gamma}_{x}^{(2)}) = \hat{\boldsymbol{K}}^{(2)} - [\hat{\boldsymbol{K}}^{(2)} \boldsymbol{Z}^{(2)^{T}} \boldsymbol{V} (\hat{\boldsymbol{\theta}}_{(p)})^{-1} \boldsymbol{Z}^{(2)} \hat{\boldsymbol{K}}^{(2)}],$$

$$\hat{\boldsymbol{\gamma}}_{t-x}^{(3)} = \hat{\boldsymbol{K}}^{(3)} \boldsymbol{Z}^{(3)^{T}} \boldsymbol{V} (\hat{\boldsymbol{\theta}}_{(p)})^{-1} (\boldsymbol{Y} - \boldsymbol{T} \hat{\boldsymbol{\beta}}_{(p)}),$$

$$\operatorname{Var}(\boldsymbol{\gamma}_{t-x}^{(3)}) = \hat{\boldsymbol{K}}^{(3)} - [\hat{\boldsymbol{K}}^{(3)} \boldsymbol{Z}^{(3)^{T}} \boldsymbol{V} (\hat{\boldsymbol{\theta}}_{(p)})^{-1} \boldsymbol{Z}^{(3)} \hat{\boldsymbol{K}}^{(3)}].$$
(3.10)

The linear fixed effects estimator $\hat{\beta}$ and its variance $Var(\beta)$ in the proposed model is

$$\hat{oldsymbol{eta}} = (oldsymbol{T}^T oldsymbol{V} (\hat{oldsymbol{ heta}}_{(p)})^{-1} oldsymbol{T})^{-1} oldsymbol{T}^T oldsymbol{V} (\hat{oldsymbol{ heta}}_{(p)})^{-1} oldsymbol{Y},$$
 $ext{Var}(oldsymbol{eta}) = \hat{\sigma}_{(p)}^2 oldsymbol{I} (oldsymbol{T}^T oldsymbol{V} (\hat{oldsymbol{ heta}}_{(p)})^{-1} oldsymbol{T})^{-1}.$

We lastly combine all the estimated components to obtain the complete matrix form of the estimated mean of the proposed model, i.e.

$$\hat{m{Y}} = m{T}\hat{m{eta}} + m{Z}^{(1)}\hat{m{\gamma}}_{m{x}}^{(1)} + m{Z}^{(2)}\hat{m{\gamma}}_{m{x}}^{(2)} + m{Z}^{(3)}\hat{m{\gamma}}_{m{t-x}}^{(3)},$$

and the variance of the estimated mean in the proposed model is

$$\operatorname{Var}(\boldsymbol{Y}) = \boldsymbol{T}\operatorname{Var}(\boldsymbol{\beta})\boldsymbol{T}^T + \boldsymbol{Z}^{(1)}\operatorname{Var}(\boldsymbol{\gamma}_{\boldsymbol{x}}^{(1)})\boldsymbol{Z}^{(1)}^T + \boldsymbol{Z}^{(2)}\operatorname{Var}(\boldsymbol{\gamma}_{\boldsymbol{x}}^{(2)})\boldsymbol{Z}^{(2)}^T + \boldsymbol{Z}^{(3)}\operatorname{Var}(\boldsymbol{\gamma}_{\boldsymbol{t}-\boldsymbol{x}}^{(3)})\boldsymbol{Z}^{(3)}^T + \hat{\sigma}_{(p)}^2\boldsymbol{I}.$$

3.2.3 Out-of-sample forecasts and the prediction intervals

In the proposed model, we can extrapolate a h-step forecast of the logit of the initial mortality rate from the last observed calendar year t_n to the calendar year t_{n+h} by extending the row of covariate matrices $\boldsymbol{T}, \boldsymbol{Z}^{(1)}, \boldsymbol{Z}^{(2)}$ from the size of $n \times m$ to $(n+h) \times m$ with $[1_{n+1}, 1_{n+2}, \dots, 1_{n+h}]^T$, new input $[t_{n+1}, t_{n+2}, \dots, t_{n+h}]^T$ and reconstructing $\boldsymbol{Z}^{(3)}$ as a new $((n+h) \times m) \times (n+h+m-1)$ cohort pattern dummy covariate matrix in Equation (3.3) denoted by $\boldsymbol{T}^*, \boldsymbol{Z}^{*(1)}, \boldsymbol{Z}^{*(2)}, \boldsymbol{Z}^{*(3)}$, such that

$$\hat{m{Y}}^* = m{T}^* \hat{m{eta}} + m{Z}^{*(1)} \hat{m{\gamma}}_{m{x}}^{(1)} + m{Z}^{*(2)} \hat{m{\gamma}}_{m{x}}^{(2)} + m{Z}^{*(3)} \hat{m{\gamma}}_{m{t+h-x}}^{(3)}$$

where

$$\hat{\gamma}_{t+h-x}^{(3)} = \hat{K}^{*(3)} Z^{(3)T} V(\hat{\theta}_{(p)})^{-1} (Y - T\hat{\beta}), \tag{3.11}$$

and $\hat{\pmb{K}}^{*(3)}$ is the size of $(n+h+m-1)\times(n+m-1)$ covariance matrix for extrapolating $\hat{\pmb{\gamma}}_{t-x}^{(3)}$ to h-step ahead , i.e.

$$\hat{\boldsymbol{K}}^{*(3)} = \hat{c}_{(p)}^{2} \exp \left(- \begin{bmatrix} \frac{((t_{1} - x_{m}) - (t_{1} - x_{m}))^{2}}{2\hat{s}_{(p)}} & \frac{((t_{1} - x_{m}) - (t_{2} - x_{m}))^{2}}{2\hat{s}_{(p)}} & \cdots & \frac{((t_{1} - x_{m}) - (t_{n} - x_{1}))^{2}}{2\hat{s}_{(p)}} \\ \frac{((t_{2} - x_{m}) - (t_{1} - x_{m}))^{2}}{2\hat{s}_{(p)}} & \frac{((t_{2} - x_{m}) - (t_{2} - x_{m}))^{2}}{2\hat{s}_{(p)}} & \cdots & \frac{((t_{2} - x_{m}) - (t_{n} - x_{1}))^{2}}{2\hat{s}_{(p)}} \\ \vdots & \vdots & \ddots & \vdots \\ \frac{((t_{n+h} - x_{1}) - (t_{1} - x_{m}))^{2}}{2\hat{s}_{(p)}} & \frac{((t_{n+h} - x_{1}) - (t_{2} - x_{m}))^{2}}{2\hat{s}_{(p)}} & \cdots & \frac{((t_{n+h} - x_{1}) - (t_{n} - x_{1}))^{2}}{2\hat{s}_{(p)}} \end{bmatrix} \right).$$

The h-step out-of-sample forecast variance by the proposed model is

$$\operatorname{Var}(\boldsymbol{Y}^*) = \boldsymbol{T}^* \operatorname{Var}(\boldsymbol{\beta}) \boldsymbol{T}^{*T} + \boldsymbol{Z}^{*(1)} \operatorname{Var}(\boldsymbol{\gamma}_{\boldsymbol{x}}^{(1)}) \boldsymbol{Z}^{*(1)T} + \boldsymbol{Z}^{*(2)} \operatorname{Var}(\boldsymbol{\gamma}_{\boldsymbol{x}}^{(2)}) \boldsymbol{Z}^{*(2)T} + \boldsymbol{Z}^{*(3)} \operatorname{Var}(\boldsymbol{\gamma}_{\boldsymbol{t+h-x}}^{(3)}) \boldsymbol{Z}^{*(3)T} + \hat{\sigma}_{(p)}^2 \boldsymbol{I},$$

where

$$Var(\boldsymbol{\gamma}_{t+h-x}^{(3)}) = \hat{\boldsymbol{K}}^{**(3)} - \hat{\boldsymbol{K}}^{**(3)} \boldsymbol{Z}^{(3)T} \boldsymbol{V}(\hat{\boldsymbol{\theta}}_{(p)})^{-1} \boldsymbol{Z}^{(3)} \hat{\boldsymbol{K}}^{**(3)},$$

and $\hat{\boldsymbol{K}}^{**(3)}$ is the size of $(n+h+m-1)\times(n+h+m-1)$ covariance matrix, i.e.

$$\hat{\boldsymbol{K}}^{**(3)} = \hat{c}_{(p)}^{2} \exp \left(- \begin{bmatrix} \frac{((t_{1} - x_{m}) - (t_{1} - x_{m}))^{2}}{2\hat{s}_{(p)}} & \frac{((t_{1} - x_{m}) - (t_{2} - x_{m}))^{2}}{2\hat{s}_{(p)}} & \cdots & \frac{((t_{1} - x_{m}) - (t_{n+h} - x_{1}))^{2}}{2\hat{s}_{(p)}} \\ \frac{((t_{2} - x_{m}) - (t_{1} - x_{m}))^{2}}{2\hat{s}_{(p)}} & \frac{((t_{2} - x_{m}) - (t_{2} - x_{m}))^{2}}{2\hat{s}_{(p)}} & \cdots & \frac{((t_{2} - x_{m}) - (t_{n+h} - x_{1}))^{2}}{2\hat{s}_{(p)}} \\ \vdots & \vdots & \ddots & \vdots \\ \frac{((t_{n+h} - x_{1}) - (t_{1} - x_{m}))^{2}}{2\hat{s}_{(p)}} & \frac{((t_{n+h} - x_{1}) - (t_{2} - x_{m}))^{2}}{2\hat{s}_{(p)}} & \cdots & \frac{((t_{n+h} - x_{1}) - (t_{n+h} - x_{1}))^{2}}{2\hat{s}_{(p)}} \end{bmatrix} \right)$$

With the normality assumptions on the model error and the estimated $\text{Var}(\boldsymbol{Y}^*)$, a $100(1-\alpha)\%$ prediction interval for $\hat{\boldsymbol{Y}}^*$ can be calculated as $\hat{\boldsymbol{Y}}^* \pm z_\alpha (\text{diag}(\text{Var}(\boldsymbol{Y}^*)))^{1/2}$, where z_α is the $(1-\alpha/2)$ quantile of the standard normal distribution.

4 Applications

In this section, we demonstrate the usefulness of the proposed model by modelling and fore-casting two sets of sex-specific empirical mortality data. We apply the proposed model to the sex-specific mortality data of Japan for illustration purposes first, then compare and evaluate the quality of the fitted sex-specific mortality curves by the proposed approach with the CBD model using sex-specific mortality data of ten different developed countries.

4.1 Male mortality data

The male mortality data of Japan is available from the year 1947 to the year 2016 (70 years in total) from the Human Mortality Database (2020). The database consists of the age-specific male central mortality rate by a single calendar year of age up to 110 years old. Given that the CBD model is designed in particular for annuities and pensions schemes for older people, we restrict the numerical examples for the same examined age groups from age 60 to age 89 (30 age groups in total) as the CBD model (Cairns et al., 2009).

We convert the central mortality rate to the initial mortality rate by Equation (2.1) and present the observed logit initial male mortality rates as univariate time series with 5-year age intervals in Figure 4.1a and the observed logit initial male mortality curves from age 60 to age 89 from the year 1947 to the year 2016 in Japan in Figure 4.1b. We can see that there is a general decrease in male mortality rates among all the selected age groups during the examined period. The changing patterns of the time-series male mortality rates look reasonably similar among all the selected groups over the examined period in Figure 4.1a. Figure 4.1b presents

the same set of data from the age side as a bunch of the mortality curves in a time-ordering indicated by the colours of the rainbow from red to violet. Its vertical pattern shows the general trends and variations of the observed initial male mortality rates across the examined period. We can see that the historical male mortality curves move downwards over time in general, due primarily to the advances in medical technology.

4.2 Male mortality modelling and forecasting

As the demonstration, we aim to display 10-years-ahead out-of-sample forecasts of the male mortality rates. We first split the dataset into a training dataset with the observed mortality rates from the year 1947 to the year 2006 and a test dataset with the remaining observed mortality data from the year 2007 to the last sample data in the year 2016.

We fit the male mortality data in the training dataset into the proposed model stated in Equation (3.3). The mean components and random components of the proposed model can be estimated as discussed in Section 3.2. Thanks to the age group dependency design in the random components of the proposed model, we can observe how the mortality rates in different age groups correlate with each other from the estimated random effects intercept coefficients and the estimated random effects slope coefficients stated in Equation (3.8) and Equation (3.9) with the 95% confidence intervals in Figure 4.2a and 4.2b. We can see that they are both increasing along with the increase in age, indicating that age is a key factor to increase the male mortality rate. Figure 4.2c presents the estimated random cohort effects coefficients stated in Equation (3.10). The shape of the estimated random cohort effects coefficients reflects the improvements or deteriorations of the male mortality among groups of people born within the same year. It shows that there is a significant improvement in mortality for those groups of people born in between the years 1880 to 1900, while a downturn happened for those groups of people born in around the years 1910 to 1920 in Japan. This may be due to the fact that this group of people

were sent to the main army force in the Second World War. We then extrapolate the estimated random cohort effects coefficients for a 10-years-ahead out-of-sample forecast using (3.11) as shown in Figure 4.2c. Figure 4.3 presents the predicted logit initial mate mortality rates of some selected age groups by the proposed method. We can see that the proposed model can capture the linear patterns of the logit initial mate mortality rates accurately with no significant misprediction. Figure 4.4 gives an example of the 10-years-ahead forecast results of the logit initial mate mortality curves from age 60 to age 89 (with RMSE = 0.0590) with 95% prediction intervals by the proposed approach for the year 2016 based on the observations from 1947 to 2006 in Japan. The root mean square error (RMSE) here is defined as

RMSE =
$$\sqrt{\frac{1}{30} \sum_{j=1}^{30} \left(y_{x_j, t_{2016}} - \hat{y}_{x_j, t_{2016}} \right)^2}$$
,

where $y_{x_j,t_{2016}}$ is the logit initial male mortality rate aged x_j in the year 2016.

4.3 Female mortality data

We move to the second case study of modelling and forecasting female mortality data. Female mortality data of Japan are also available from the year 1947 to the year 2016 in the Human Mortality Database (2020). We maintain the same selection for the age groups and also convert the central female mortality rate to the initial female mortality rate by Equation (2.1) as in the male mortality case for demonstration in this section.

We present the historical mortality data of Japan as separate univariate time series of the logit initial female mortality rates with 5-year age intervals in Figure 4.5a and as the logit initial mortality curves from age 60 to age 89 from the year 1947 to the year 2016 in a time-ordering indicated by the colours of the rainbow from red to violet in Figure 4.5b. We can see that the downward movement of the time-series female mortality looks fairly similar among all the selected groups as well as the patterns of the male mortality over the examined period in Figure

4.5a. Figure 4.5b presents the same set of data from the age side as a bunch of the mortality curves in a time-ordering indicated by the colours of the rainbow from red to purple. Its vertical pattern shows the general trends and variations of the observed initial female mortality rates across the examined period. We can also see that the historical female mortality curves move downwards over time in general due mainly to the advances in medical technology and longer longevity as in the case of male mortality discussed in the previous section.

4.4 Female mortality modelling and forecasting

For the task of female mortality modelling and forecasting, we again attempt to make 10-yearsahead out-of-sample forecasts of the logit initial female mortality rates for demonstration and maintain the same setting for the split of dataset as for the male mortality case in this section.

The female mortality data in the training dataset is fitted into the proposed model stated in Equation (3.3). Figure 4.6a and Figure 4.6b demonstrate the estimated random effects intercept coefficients and the estimated random effects slope coefficients with the 95% confidence intervals for the fitted female mortality data. We can see that they also have increasing patterns along with the increase in age, reflecting that age is also an essential element to increase the female mortality rate in Japan. Figure 4.6c presents the estimated random cohort effects coefficients stated in Equation (3.10). The shape of the estimated random cohort effects coefficients reflects the improvements or deteriorations of the female mortality among groups of people born within the same year. Similar to the pattern of the estimated random cohort effects coefficients in the male mortality case, there is also a significant improvement in female mortality for those groups of people born in between the years 1880 to 1900, while a downturn happened for those groups of people born in around the years 1910 to 1920 in Japan. We then extrapolate the estimated random cohort effects coefficients for a 10-years-ahead out-of-sample forecast using Equation (3.11) as shown in Figure 4.6c. Figure 4.7 presents the predicted logit initial female mortal-

ity rates of the selected age groups by the proposed model. We can observe that the proposed model can catch the linear patterns of the logit initial female mortality rates reasonably well with no significant mistake. Figure 4.8 provides the demonstration of the 10-years-ahead forecast results of the logit initial female mortality curves from age 60 to age 89 (with RMSE = 0.0842) with the 95% prediction intervals by the proposed model for the year 2016 based on the observations from 1947 to 2006 in Japan.

4.5 Forecast accuracy evaluations and comparisons with the CBD model

We now compare and evaluate the forecast performance of the proposed mixed-effects time series model with the CBD model reviewed in Section 2. In order to have a comprehensive investigation of the forecast accuracy among these two models, we consider ten other developed countries for which data are also available in the Human Mortality Database (2020). We restrict data periods of all selected countries commencing in the year 1947 up to the year 2016 (70 years in total) for a unified purpose. We examine and quantify the forecasting performance of the models by the rolling window analysis, which is frequently used for assessing the consistency of a model's forecasting ability by rolling a fixed size prediction interval (window) throughout the observed period (Zivot & Wang, 2007). We hold the sample data from the initial year up to the year t_l , where $t_l < t_n$, as holdout samples and produce the forecast for the t_{l+h} year where h is the forecast horizon. The forecasts errors are then determined by comparing the out-ofsample forecast results with the actual data. We increase one rolling-window (1 year ahead) in year t_{l+1} to make the same procedure again for the year t_{l+1+h} until the rolling-window analysis covers all available data in year t_n . We consider four different forecast horizons (h = 5, 10, 15and 20) with ten sets of rolling-window to examine the short-term, the mid-term, and the longterm forecast abilities of the models. In our mortality rolling-window experiments, the RMSE is defined as

$$\mathrm{RMSE}_c^{(i)}(h) = \sqrt{\frac{1}{10 \times 30} \sum_{w=0}^{9} \sum_{j=1}^{30} \left(y_{x_j, t_{l+w+h}}^{(i)} - \hat{y}_{x_j, t_{l+w+h}}^{(i)} \right)^2},$$

where c is the selected country, w is the index of the rolling-window sets, i is for male (i = M) and for female (i = F), and j is the index of the examined age groups covering from age 60 to age 89.

Table 4.1 presents the average RMSEs of ten sets of the rolling window analysis across the ten selected countries in four different forecast horizons in the male and female mortality curves fitting experiments. The back-testing results confirm that the forecasting performances and accuracy of the proposed model are much more desirable than the CBD model⁴. Among all the ten selected countries and the four different forecast horizons, the proposed model scored the majority of the lowest RMSEs in both genders, different countries and forecast horizons in the numerical experiment.

5 Discussion and conclusion remarks

In this article, we have introduced a novel mortality model under the time-series and mixedeffects structure. We have presented the formulation, the model assumptions and the estimation of the parameters as well as the differences between the CBD model and the proposed model. We lastly compared the forecasting abilities among the two models using the rolling window analysis across the mortality data of ten selected countries. The proposed mixed effects model has four remarkable advantages over the CBD model as summarised below.

1. Circumventing the age-period-cohort identification problem

The proposed mixed effects model provides an alternative way to avoid the age-period-

⁴The CBD model was implemented using *R* package '*StMoMo*' in the numerical experiment (Villegas et al., 2015).

cohort identification problem when estimating the model cohort effects parameters. Unlike the CBD model which estimates the model cohort effects parameters as the fixed-effects parameters by placing the specified constraints through the iterative optimisation process, the proposed model under the mixed-effects structure can produce a unique best fitting solution without the need for introducing any pre-defined constraints on the model cohort effects parameters. It is because the model cohort effects parameters are treated as random variables with their own specific distributions. The structure of the proposed model also allows us to examine how different age groups correlate with each other and disclose underlying mortality information about the age groups correlation patterns in a more compendious fashion than the CBD model.

2. Unified time series framework for out-of-sample extrapolation

The CBD model obtains the estimates of the model parameters under a fixed-effects regression based approach first, then applies the random walk with drift processes method to do the model coefficients extrapolation in the second step. In contract, our proposed model can extrapolate the out-of-sample mortality rates under a unified single step framework. Indeed, De Jong & Tickle (2006), Sweeting (2011), Fung et al. (2017) and Li & O'Hare (2017) doubt about the appropriateness of using the random walk with drift processes method to extrapolate the coefficients of the CBD model as a two-step approach. Leng & Peng (2016) also argue that the two-steps approach is a somewhat ad-hoc procedure, and it would be more ideal to perform the estimation and the extrapolation under a consistent and rigorous single universal framework from the statistical point of view. The proposed model in this article aims to provide the unified time series framework and avoids any potential pitfalls using the two-step estimation procedure that the CBD model may fall.

3. Natural confidence intervals under the normal distribution assumption

The CBD model is constructed based on the Poisson distribution assumption, and it is difficult to quantify the uncertainties of the estimated model parameters due to the equal Poisson mean and variance and the over-dispersion problems. However, the proposed model can provide natural confidence intervals that include the estimated model parameters uncertainties and the prediction intervals for the out-of-sample extrapolation given that the proposed model is established under the Bayesian paradigm with the normal distribution assumption. The ability to quantifying the parameter risks can enhance the reliability of the prediction, and this ability is especially practical for valuing the uncertainties for life insurance portfolios and pension schemes in the insurance industry.

4. Improved forecasting accuracy

The forecasting performance of the proposed model is better than the CBD model. In our window-rolling experiments across the mortality data of the ten developed countries, the accuracies of the predicted mortality curves are significantly improved by the proposed model in short-term, mid-term and long-term forecasting. The improvements may be mainly due to the time-series and mixed-effects framework of the proposed model, which can directly extrapolate the data forward without the need of placing any extra assumptions on the model parameters.

Despite the advantages of the proposed CBD model listed above, both our model and the CBD model only work when there is a linear pattern in the latter part of the mortality curve above the pension age. Neither of them are capable of handling any non-linear mortality patterns for young ages. Although some attempts have been made to extend the existing CBD model design while keeping its simplicity to cover the whole age range for mortality modelling, see, for example, Plat (2009), Cairns et al. (2009), further research is still needed to consider about

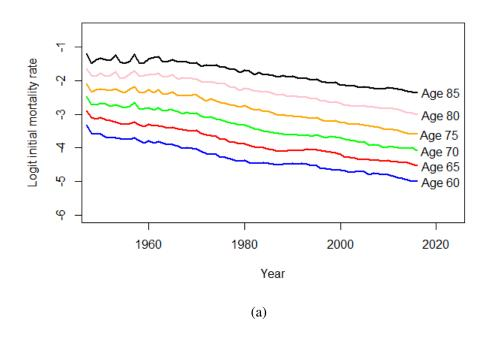
extending the proposed model with more factors which can handle more comprehensive age ranges or embedding some time weightings approaches in the model estimation procedure so that it can capture more recent mortality patterns for better forecasting performance.

References

- Cairns, A. J., Blake, D., & Dowd, K. (2006). A two-factor model for stochastic mortality with parameter uncertainty: Theory and calibration. *Journal of Risk and Insurance*, 73(4), 687–718.
- Cairns, A. J., Blake, D., Dowd, K., Coughlan, G. D., Epstein, D., Ong, A., & Balevich, I. (2009). A quantitative comparison of stochastic mortality models using data from England and Wales and the United States. *North American Actuarial Journal*, *13*(1), 1–35.
- Currie, I. D. (2016). On fitting generalized linear and non-linear models of mortality. *Scandinavian Actuarial Journal*, 2016(4), 356–383.
- De Jong, P., & Tickle, L. (2006). Extending Lee–Carter mortality forecasting. *Mathematical Population Studies*, *13*(1), 1–18.
- Dickson, D. C., Hardy, M., Hardy, M. R., & Waters, H. R. (2013). *Actuarial Mathematics for Life Contingent Risks*. Cambridge University Press.
- Fung, M. C., Peters, G. W., & Shevchenko, P. V. (2017). A unified approach to mortality modelling using state-space framework: Characterisation, identification, estimation and forecasting. *Annals of Actuarial Science*, *11*(2), 343–389.
- Haberman, S., & Renshaw, A. (2011). A comparative study of parametric mortality projection models. *Insurance: Mathematics and Economics*, 48(1), 35–55.
- Holford, T. R. (1983). The estimation of age, period and cohort effects for vital rates. *Biometrics*, 311–324.

- Human Mortality Database. (2020). University of California, Berkeley (USA), and Max Planck Institute for Demographic Research (Germany). Available online: https://www.mortality.org/. Accessed on 20 April 2020.
- Lee, R. D., & Carter, L. R. (1992). Modeling and forecasting US mortality. *Journal of the American Statistical Association*, 87(419), 659–671.
- Leng, X., & Peng, L. (2016). Inference pitfalls in Lee–Carter model for forecasting mortality. *Insurance: Mathematics and Economics*, 70, 58–65.
- Li, H., & O'Hare, C. (2017). Semi-parametric extensions of the Cairns–Blake–Dowd model: A one-dimensional kernel smoothing approach. *Insurance: Mathematics and Economics*, 77, 166–176.
- Li, H., O'Hare, C., & Vahid, F. (2016). Two-dimensional kernel smoothing of mortality surface: An evaluation of cohort strength. *Journal of Forecasting*, *35*(6), 553–563.
- Murphy, M. (2009). The 'Golden Generations' in historical context. *British Actuarial Journal*, 151–184.
- Murphy, M. (2010). Reexamining the dominance of birth cohort effects on mortality. *Population and Development Review*, *36*(2), 365–390.
- O'Brien, R. M. (2014). Estimable functions in age-period-cohort models: A unified approach. *Quality & Quantity*, 48(1), 457–474.
- O'Brien, R. M. (2017). Mixed models, linear dependency, and identification in age-period-cohort models. *Statistics in Medicine*, *36*(16), 2590–2600.
- Plat, R. (2009). On stochastic mortality modeling. *Insurance: Mathematics and Economics*, 45(3), 393–404.
- Renshaw, A. E., & Haberman, S. (2003). Lee–Carter mortality forecasting with age-specific enhancement. *Insurance: Mathematics and Economics*, *33*(2), 255–272.

- Sweeting, P. J. (2011). A trend-change extension of the Cairns-Blake-Dowd model. *Annals of Actuarial Science*, 5(2), 143–162.
- Villegas, A., Kaishev, V. K., & Millossovich, P. (2015). StMoMo: An *R* package for stochastic mortality modelling. In *7th Australasian Actuarial Education and Research Symposium*.
- Willets, R. C. (2004). The cohort effect: insights and explanations. *British Actuarial Journal*, 833–898.
- Zivot, E., & Wang, J. (2007). *Modeling Financial Time Series with S-Plus*® (Vol. 191). Springer Science & Business Media.



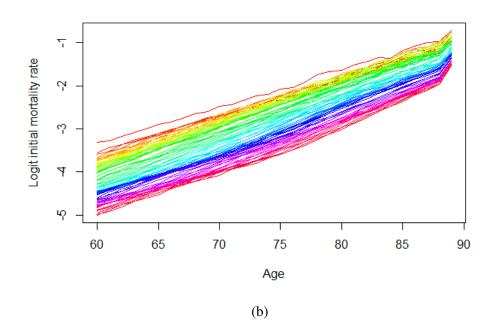


Figure 4.1: (a) Univariate time series of the observed logit initial male mortality rates with 5-year age intervals and (b) the logit initial male mortality curves from age 60 to age 89 from the year 1947 to the year 2016 in Japan.

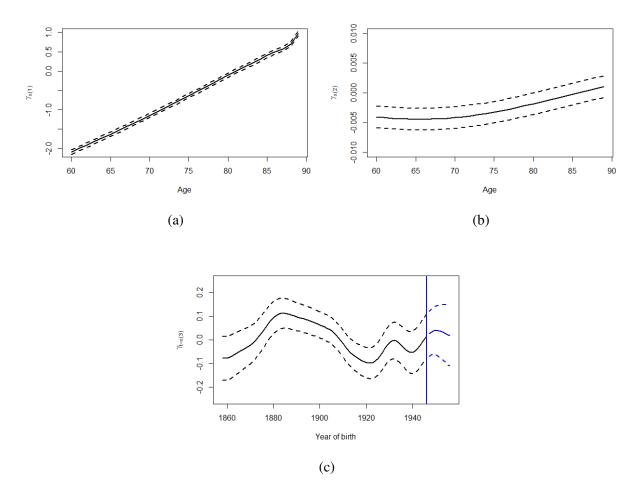


Figure 4.2: (a) Estimated random effects intercept coefficients, (b) the estimated random effects slope coefficients and (c) the estimated random cohort effects coefficients using the observed logit initial male mortality rates of Japan from the year 1947 to the year 2006. Dashed lines are the 95% confidence intervals and the vertical line indicates the start point of the 10-years-ahead forecasts of the estimated random cohort effects coefficients.

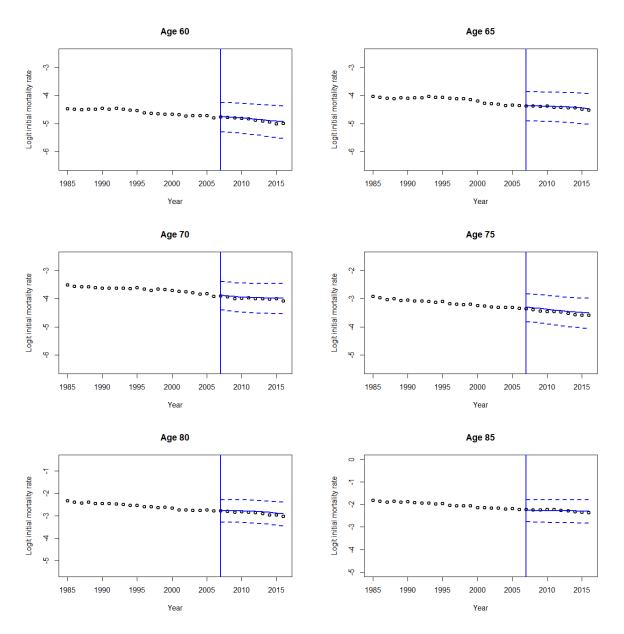


Figure 4.3: Predicted logit initial male mortality rates of the selected age groups from ages 60 to 89 with 5-year age intervals using the proposed model from the year 2007 to the year 2016 based on the observations from the year 1947 to the year 2006 in Japan. The circles are the observed values, the solid lines are the predictions, and the dashed lines are the 95% prediction intervals. The vertical line indicates the start point of the predictions.

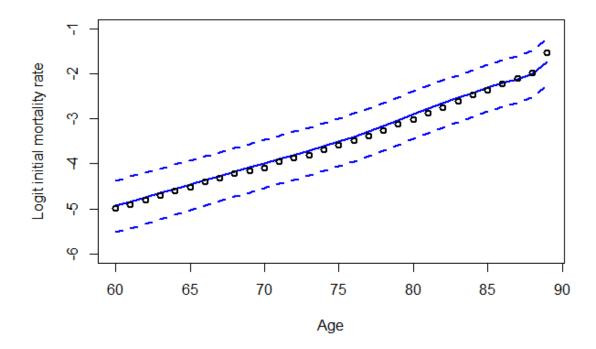
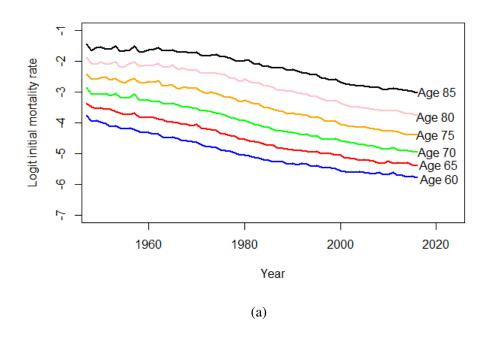


Figure 4.4: Predicted logit initial male mortality curve (with RMSE = 0.0793) from age 60 to age 89 with the 95% prediction intervals using the proposed model for the year 2016 based on the observations from the year 1947 to the year 2006 in Japan. The circles are the observed logit initial male mortality rates, the solid line is the prediction and the dashed lines are the 95% prediction intervals.



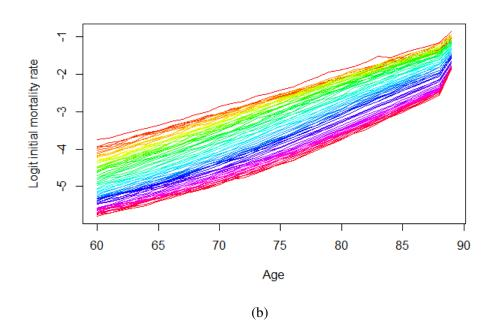


Figure 4.5: (a) Univariate time series of the observed logit initial female mortality rates with 5-year age intervals and (b) the logit initial female mortality curves from age 60 to age 89 from the year 1947 to the year 2016 in Japan.

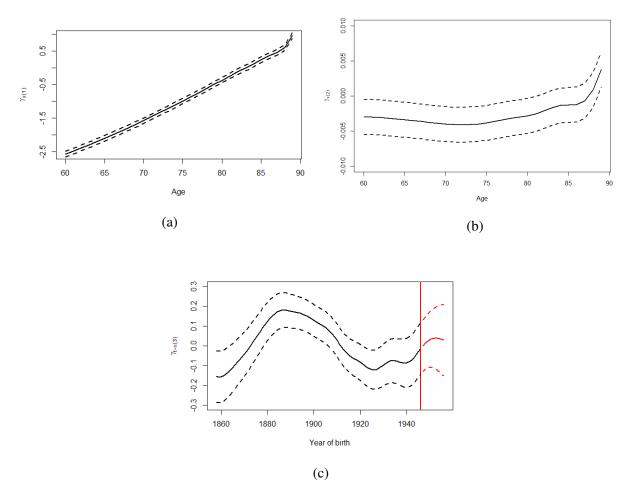


Figure 4.6: (a) Estimated random effects intercept coefficients, (b) the estimated random effects slope coefficients and (c) the estimated cohort effects coefficients using the observed logit initial female mortality rates of Japan from the year 1947 to the year 2006. Dashed lines are the 95% confidence intervals and the vertical line indicates the start point of the 10-years-ahead forecasts of the estimated random cohort effects coefficients.

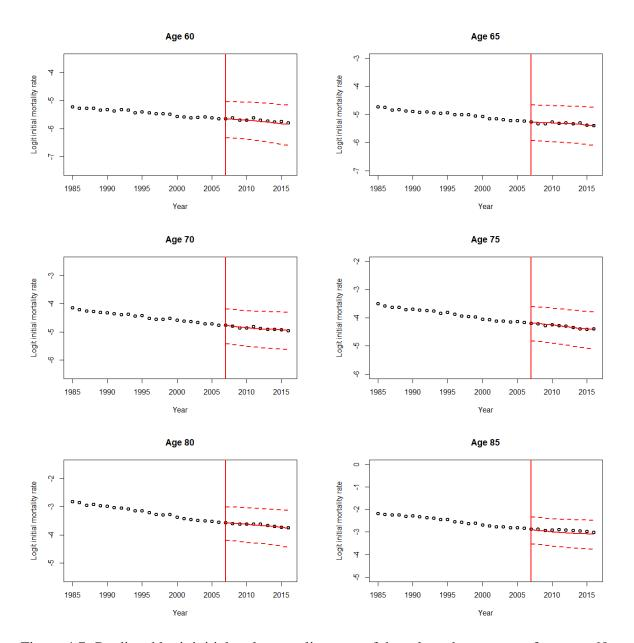


Figure 4.7: Predicted logit initial male mortality rates of the selected age groups from age 60 to age 89 with 5-year age intervals using the proposed model from the year 2007 to the year 2016 based on the observations from the year 1947 to the year 2006 in Japan. The circles are the observed values, the solid lines are the predictions and the dashed lines are the 95% prediction intervals. The vertical line indicates the start point of the predictions.

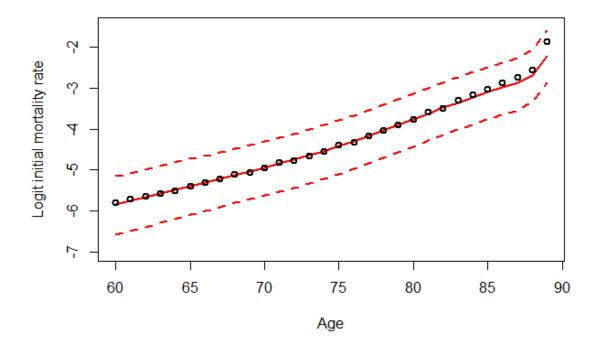


Figure 4.8: Predicted logit initial female mortality curve (with RMSE = 0.0842) from age 60 to age 89 with the 95% prediction intervals using the proposed model for the year 2016 based on the observations from the year 1947 to the year 2006 in Japan. The circles are the observed logit initial female mortality rates, the solid line is the prediction and the dashed lines are the 95% prediction intervals.

Country	CBD model			Proposed model		
	M	F	<u>M+F</u>	M	F	<u>M+F</u>
h = 5						
Australia	0.1174	0.1603	0.1388	0.1398	0.1103	0.1251
Belgium	0.1039	0.1547	0.1293	0.0783	0.0557	0.0670
Canada	0.0938	0.1607	0.1272	0.0481	0.0547	0.0514
France	0.1929	0.2614	0.2271	0.0780	0.0580	0.0680
Italy	0.1076	0.1544	0.1310	0.1109	0.0624	0.0866
Japan	0.1229	0.1659	0.1444	0.0682	0.0759	0.0721
Netherlands	0.1219	0.1769	0.1494	0.1050	0.1423	0.1236
Spain	0.1106	0.1570	0.1338	0.0839	0.0744	0.0792
UK	0.1381	0.1280	0.1330	0.1237	0.0584	0.0911
USA	0.1065	0.1729	0.1397	0.0558	0.0600	0.0579
Average	0.1215	0.1692	0.1454	0.0892	0.0752	0.0822
h = 10						
Australia	0.1644	0.2270	0.1957	0.1660	0.1635	0.1648
Belgium	0.1196	0.2054	0.1625	0.1153	0.1467	0.1310
Canada	0.1337	0.2467	0.1902	0.1042	0.1174	0.1108
France	0.3247	0.4384	0.3815	0.0787	0.0846	0.0817
Italy	0.1562	0.2079	0.1821	0.1194	0.0731	0.0963
Japan	0.1756	0.2093	0.1925	0.1023	0.1134	0.1078
Netherlands	0.1580	0.2572	0.2076	0.1504	0.1765	0.1635
Spain	0.1563	0.2234	0.1899	0.1191	0.1039	0.1115
ÜK	0.1915	0.1812	0.1864	0.1360	0.1493	0.1426
USA	0.1735	0.2953	0.2344	0.1308	0.0742	0.1025
Average	0.1754	0.2492	0.2123	0.1222	0.1203	0.1213

Table 4.1: The average RMSEs in ten sets of the rolling-windows analysis of the predicted mortality curves across the ten selected countries using the CBD model and the proposed model. The minimal forecast errors are highlighted, and the lowest averaged forecast errors among models in different forecast horizons are highlighted in bold.

Country	CBD model			Proposed model		
	M	F	$\frac{M+F}{2}$	M	F	$\frac{M+F}{2}$
h = 15						
Australia	0.2373	0.2679	0.2526	0.2899	0.2039	0.2469
Belgium	0.1412	0.2126	0.1769	0.1373	0.1286	0.1330
Canada	0.1753	0.2851	0.2302	0.1373	0.0631	0.1002
France	0.3858	0.4793	0.4326	0.1672	0.1009	0.1340
Italy	0.2212	0.2460	0.2336	0.2446	0.0899	0.1672
Japan	0.2271	0.2268	0.2270	0.1504	0.1079	0.1292
Netherlands	0.2454	0.2680	0.2567	0.2276	0.1969	0.2123
Spain	0.2092	0.2848	0.2470	0.1536	0.1360	0.1448
UK	0.2698	0.2300	0.2499	0.1540	0.2130	0.1835
USA	0.2056	0.3218	0.2637	0.1153	0.0523	0.0838
Average	0.2318	0.2822	0.2570	0.1777	0.1292	0.1535
$\frac{h=20}{}$						
Australia	0.3387	0.2887	0.3137	0.3878	0.2783	0.3330
Belgium	0.1835	0.2280	0.2057	0.2052	0.1462	0.1757
Canada	0.2250	0.2680	0.2465	0.3091	0.0582	0.1836
France	0.4166	0.4128	0.4147	0.1876	0.1287	0.1582
Italy	0.3180	0.3037	0.3109	0.2875	0.1204	0.2039
Japan	0.2945	0.2127	0.2536	0.2551	0.1258	0.1904
Netherlands	0.3457	0.2922	0.3190	0.3111	0.1729	0.2420
Spain	0.2628	0.3555	0.3091	0.1972	0.1787	0.1880
ŪK	0.3711	0.2950	0.3331	0.2866	0.2538	0.2702
USA	0.2173	0.2906	0.2539	0.1706	0.0532	0.1119
Average	0.2973	0.2947	0.2960	0.2598	0.1516	0.2057

Table 4.1: (continued) The average RMSEs in ten sets of the rolling-windows analysis of the predicted mortality curves across the ten selected countries using the CBD model and the proposed model. The minimal forecast errors are highlighted, and the lowest averaged forecast errors among models in different forecast horizons are highlighted in bold.